A critical assessment of the line tension determined by the modified Young's equation

Jun Zhang, Pengfei Wang, Matthew K. Borg, Jason M. Reese, and Dongsheng Wen

Citation: Physics of Fluids **30**, 082003 (2018); doi: 10.1063/1.5040574
View online: https://doi.org/10.1063/1.5040574
View Table of Contents: http://aip.scitation.org/toc/phf/30/8
Published by the American Institute of Physics

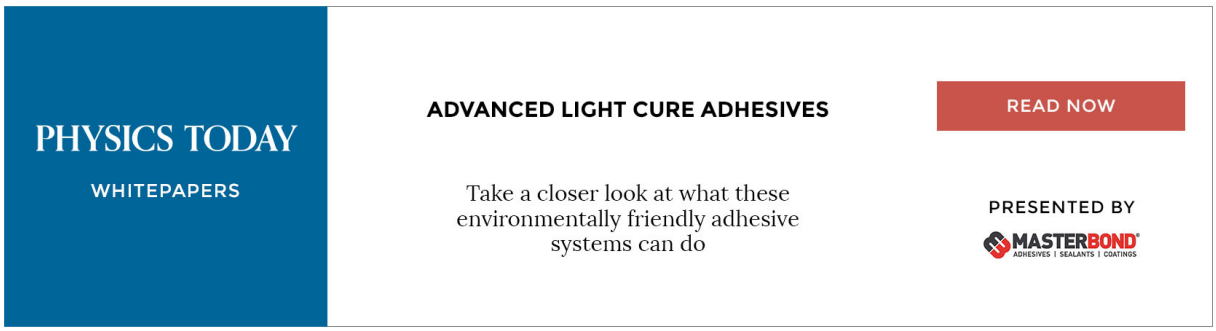

A critical assessment of the line tension determined by the modified Young's equation

Jun Zhang,[1,a)] Pengfei Wang,[1] Matthew K. Borg,[2] Jason M. Reese,[2] and Dongsheng Wen[1,3]
[1]*School of Aeronautic Science and Engineering, Beihang University, Beijing 100191, China*
[2]*School of Engineering, University of Edinburgh, Edinburgh EH9 3FB, United Kingdom*
[3]*School of Chemical and Process Engineering, University of Leeds, Leeds LS2 9JT, United Kingdom*

(Received 18 May 2018; accepted 13 July 2018; published online 8 August 2018)

Although the modified Young's equation is frequently applied to evaluate the line tension of droplets, debate concerning the value and even the sign of the line tension is ongoing. The reason for this is that the line tension defined in the modified Young's equation is not a pure line tension but an apparent line tension, which includes the effects of the Tolman length and the stiffness coefficients. In this paper, we employ molecular dynamics (MD) to simulate three-dimensional water nanodroplets on platinum surfaces and determine their apparent line tensions by applying a linear fit to the relation of the cosine of the contact angle to the curvature of the contact line. The effects of the Tolman length and the position of the solid-liquid dividing interface on the measured line tension are investigated. On the one hand, our results elucidate the reason why MD results for line tensions are so scattered and also lend numerical support to Schimmele *et al.*'s theoretical predictions ["Conceptual aspects of line tensions," J. Chem. Phys. **127**, 164715 (2007)]. On the other hand, our MD simulation results demonstrate that the modified Young's equation is a useful tool to predict the macroscopic contact angle based on a linear fit of the measured contact angles at the nanoscale. The apparent line tension is, however, sensitive to the chosen position of the solid-liquid dividing interface. https://doi.org/10.1063/1.5040574

I. INTRODUCTION

Over the past two decades, increasing effort has been spent on understanding the behavior of droplets because of their use in a variety of engineering applications, such as ink-jet printers, spray cooling, spray combustion, and surface coating.[1,2] Most recently, research interest in nanodroplets has grown because these have their own specific wetting and evaporation properties.[3–5] Nanodroplets can provide a confined environment for nanomaterial synthesis and form novel nanostructures through liquid transition.[6,7]

The wetting of droplets of any size on solid surfaces is a fundamental phenomenon. Generally, the contact angle between the liquid-vapour interface and the solid surface is used to describe the wetting property. From a mechanical point of view, the contact angle is a balance between the surface tensions (defined as the excess free energy per unit surface of an interface separating two phases) of the solid-vapour (γ_{sv}), the solid-liquid (γ_{sl}), and the liquid-vapour (γ_{∞}) interfaces. This balance is described by the well-known Young's equation,[8]

$$\cos\,\theta_Y = \frac{\gamma_{sv} - \gamma_{sl}}{\gamma_{\infty}}, \tag{1}$$

where θ_Y is Young's contact angle at equilibrium. Although Young's equation has some limitations, such as the absence of a force balance in the direction normal to the solid surface, it has been generally accepted as describing the equilibrium wetting properties of droplets on planar, smooth, homogeneous surfaces at the macroscale.[9,10]

At the nanoscale, the validity of Young's equation remains an open question.[11–13] There is evidence that the contact angle of nanodroplets on planar, smooth, homogeneous surfaces could deviate significantly from that predicted by Young's equation.[12,14–16] A reason proposed for this is that the wetting of nanodroplets is determined not only by the balance of surface tensions but also by the tension of the line where the three distinct phases meet. By analogy with surface tension, line tension is defined as the excess free energy per unit length of a three-phase contact line.[17] As the size of a droplet decreases, the relative proportion of molecules in the vicinity of the contact line increases, so the effect of line tension becomes more important. To take this into account, Young's equation has been modified to[18]

$$\cos\,\theta = \frac{\gamma_{sv} - \gamma_{sl}}{\gamma_{\infty}} - \frac{\tau}{\gamma_{\infty} a} = \cos\,\theta_Y - \frac{\tau}{\gamma_{\infty} a}, \tag{2}$$

where θ is the contact angle of nanodroplets, τ is the line tension, and a is the radius of the contact line. From Eq. (2), we can see that if the line tension is positive, droplets will present a larger contact angle than Young's angle; if the line tension is negative, droplets will present a smaller contact angle.

Although the concept of a line tension is not new,[17] its sign, magnitude, and significance are still subject to controversy. Theoretical analyses of line tension are based on calculating the free energy per unit length in the region of the three-phase contact line using either density functional

a)Electronic mail: jun.zhang@buaa.edu.cn

theory[19] or a model based on interface displacement.[20] These analyses indicate that the magnitude of the line tension is very small, from 10^{-12} to 10^{-10} J/m. Such a small magnitude makes its experimental measurement very challenging. For a review of experimental methods and results, see Ref. 21. Recently, high-resolution atomic force microscopy has also been used to measure the line tension.[22] However, the measured experimental values cover a wide range, from 10^{-12} to 10^{-5} J/m. One of the main reasons for this variation is the imperfections in solid surfaces, such as surface roughness and defects, chemical heterogeneities, and so on. Slight differences in surface properties can produce large changes in the magnitude of the line tension and even in its sign.

Molecular Dynamics (MD) has been employed to study the wetting properties of nanodroplets on surfaces, as well as the line tension behavior. The advantage of MD is that the solid surface can be constructed to be perfectly smooth and homogeneous. A popular way to measure line tension using MD is to apply a linear fit to the relation of the cosine of the measured contact angle to the radius of the contact line,[23] as given in Eq. (2). Since the seminal work using this method conducted by Werder *et al.*,[15] there have been a large number of MD results reported for the line tension of droplets. For example, Weijs *et al.*[16] investigated monatomic liquid droplets (using the simple Lennard-Jones molecular model) and determined that the line tension was negative, with a magnitude in the range 1.4×10^{-12}–1.6×10^{-11} J/m. Dutta *et al.*[24] studied the wetting properties of water on graphite and boron-nitride surfaces, and the line tensions were reported to be in the range 10^{-10}–10^{-9} J/m for temperatures from 300 to 420 K. Barisik and Beskok[25] investigated water droplets on silicon surfaces and reported line tensions from -4.5×10^{-11} to 3.5×10^{-11} J/m, depending on the wetting properties. It can be seen that the line tensions of droplets span a wide range due to the different materials of droplets and surfaces. Even when the problem setups are the same, for example, pure water droplets on graphite, the line tensions determined by different research groups using MD are quite scattered. While the magnitude is of the order of 10^{-11} J/m, the signs of the line tensions can be either positive or negative.[15,26,27]

These discrepancies in the MD simulation results are not just caused by computational errors but more importantly by the definition of the line tension itself. As pointed out by Schimmele *et al.*,[28,29] the line tension defined in the modified Young's equation is not a "pure line tension" but an "apparent line tension" that combines the pure line tension with the effects of the Tolman length and the stiffness coefficients of the contact line. The Tolman length measures the extent by which the surface tension of a small liquid droplet deviates from its planar value, and the stiffness coefficients of the contact line represent the dependence of the line tension on the contact angle and contact radius.

However, the difference between pure and apparent line tensions has not been paid much attention by previous research. Almost all reported MD results for the line tension are determined by fitting the MD data to the modified Young's equation, and so are apparent line tensions. At the nanoscale, the effects of the Tolman length and stiffness coefficients on the contact angle of droplets might be greater than the effect of the pure line tension. This is why reported line tensions by MD simulations are so scattered. Recently, Kanduč[30] employed MD to study two-dimensional cylindrical water droplets on surfaces and found that the contact angle was size dependent. This phenomenon seems counter-intuitive, as the contact line of a cylindrical droplet is straight, and consequently the line tension itself should not affect the contact angle. Kanduč[30] concluded that the size-dependence of the contact angle of cylindrical droplets is due to the effects of Tolman length and stiffness coefficients.

In this paper, we employ MD to simulate three-dimensional nanodroplets on platinum-type surfaces for both hydrophobic and hydrophilic cases, and we obtain the apparent line tension by fitting the MD data to the modified Young's equation. The effects of the Tolman length and the position of the solid-liquid dividing interface on the measured line tension are investigated separately. Our results elucidate why the reported MD results of line tensions are so scattered and give numerical support to Schimmele *et al.*'s theoretical predictions. Our results demonstrate that the modified Young's equation is a useful tool for predicting the macroscopic contact angle based on a linear fit of the measured contact angles at the nanoscale, although the line tension used in the modified Young's equation is the apparent value instead of the pure line tension.

II. SIMULATIONS AND METHODOLOGY

Molecular dynamics (MD) simulations are performed of 3D water droplets on platinum-like surfaces using the mdFoamPlus solver[31] within the OpenFOAM software, which can be downloaded freely at www.github.com/micronanoflows. The mdFoamPlus solver, which is an advance on the mdFoam solver, is a highly parallel MD code written by the authors and their collaborators. It has been validated for a variety of micro/nanoflows and multiphase flows, especially droplet wetting and evaporation.[32–35]

To prepare the pre-equilibrated water droplets, we first set up a cubic simulation box of sides 20 nm and put a small cubic box containing a certain number of water molecules in the middle of the whole region. The system is controlled at 300 K using a Berendsen thermostat and is run for 2 ns, and the water cubic box gradually becomes a sphere shape to reach a minimum energy state. In our work, five different sizes of droplets containing 2744, 4128, 5832, 8000, and 12 167 water molecules are investigated, and the equilibrated sphere radii are 2.66 nm, 3.05 nm, 3.42 nm, 3.80 nm, and 4.37 nm, respectively. After getting the pre-equilibrated water droplets, we put them on the platinum surface, as shown in Fig. 1(a). The simulation domain is a cubic box of sides 25 nm, with periodic boundary conditions applied in all three directions. The platinum substrate is constructed of 8 layers of atoms in an fcc structure with lattice constant 3.92 Å. The atoms in the bottom four layers are fixed to their equilibrated lattice sites, while the atoms in the top four layers are coupled to a Berendsen thermostat to control the temperature at 300 K throughout the simulation. Note that we do not control the temperature of water molecules in the spreading process. The Lennard-Jones (LJ) pair potential is employed for the interactions between

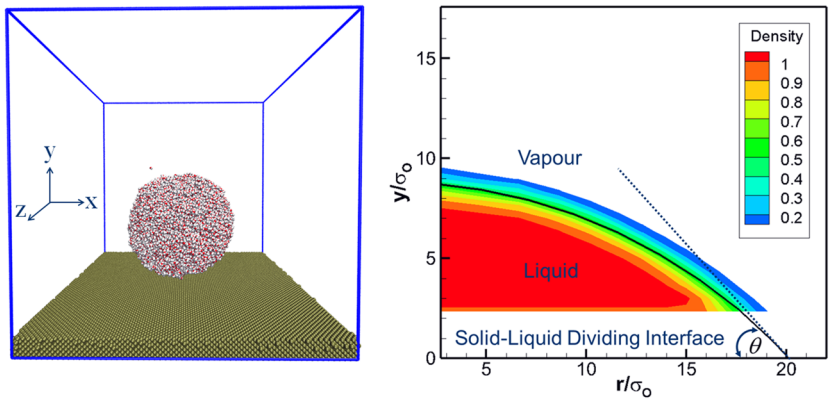

(a) (b)

FIG. 1. (a) Initial setup of the MD simulation box, including water droplet and the platinum surface and (b) density contour and contact angle measurement.

the platinum atoms, with the parameters $\epsilon_{Pt} = 66.84$ kJ mol^{-1} and $\sigma_{Pt} = 0.2471$ nm.[33]

The rigid TIP4P/2005 model is used to simulate the water molecules, as in our previous studies of water droplet wetting and evaporation.[33,34] In this model, a water molecule comprises one oxygen site (no charge), two hydrogen sites (0.5564e), and one massless site M (−1.1128e). The interactions between water molecules are both LJ potential and Coulomb forces. Specifically, the LJ potential is only applied to oxygen sites, with parameters $\epsilon_O = 0.7749$ kJ mol^{-1} and $\sigma_O = 0.3159$ nm,[36] while the Coulomb potential is applied to the sites with charges. To fix the geometry of water molecules with an O—H distance of 0.095 72 nm and an H—O—H angle of 104.52°, Hamilton's quaternions are employed.

The water-platinum interactions are based on LJ pair potentials between the oxygen atoms and the platinum atoms. The potential parameters are determined using Lorentz-Berthelot mixing rules, i.e.,

$$\sigma_{Pt-O} = \frac{\sigma_{Pt} + \sigma_O}{2}, \tag{3}$$

$$\epsilon_{Pt-O} = \lambda\sqrt{\epsilon_{Pt} \times \epsilon_O}, \tag{4}$$

where λ is a parameter used to adjust the interaction strength and hence the wetting properties. In our simulations, we choose λ to be 0.10 or 0.25 to simulate a hydrophobic surface or a hydrophilic surface, respectively.

A cell-list algorithm is used for computing pair potentials, and the Velocity Verlet algorithm is employed to update molecular velocities and positions with an integration time step of 1.67 fs. Previous studies showed that a cutoff radius of 1.2 nm without Ewald sums can provide acceptable accuracy with computational efficiency,[15,32,33] and so it is adopted in this paper. The full MD system is first run for 2 ns to produce the nanodroplet spreading on the surface and reach an equilibrium state. Then the simulation is run for another 2 ns of averaging time in order to measure the density contours and the equilibrium contact angle.

We sample the water molecules in cylindrical bins that have the defined solid-liquid dividing interface as their zero reference level and that have a normal line through the center of mass of the droplet as their reference axis. The bins are of equal volume and each extends 0.2 nm in height. To extract the contact angle from the density contours, a standard method is to fit the liquid-vapour interface to a circle;[15,33,37,38] the liquid-vapour interface is determined and captured by the points in the cylindrical bins that have half the bulk density of the liquid phase; then, a circular fit is made through these points and extrapolated to the solid-liquid dividing interface, as shown in Fig. 1(b). Note that the water density oscillates close to the solid surface so the points of the determined liquid-vapour interface below a height of $2\sigma_O$ from the solid surface are ignored in making the circular fit. The contact angle is then obtained as the angle between the tangent line to the fitting circle and the solid-liquid dividing interface. Correspondingly, the contact radius is obtained as the distance from the centre of the droplet to the intersection of the tangent line with the solid-liquid dividing interface.

III. RESULTS AND DISCUSSIONS

We study both hydrophobic and hydrophilic cases by choosing specific parameters for the water-platinum interaction strength, as explained in Sec. II. For each wetting case, five different droplets comprising 2744, 4128, 5832, 8000, and 12 167 water molecules are simulated in order to study the size-dependence of the contact angle and to determine the line tension. The solid-liquid dividing interface is first defined as the plane of the topmost solid atoms. The effects of the Tolman length and the solid-liquid dividing interface on the line tension are discussed separately in this section.

A. Effect of the Tolman length

The straightforward way to determine the line tension is using the modified Young's equation. Similar to previous MD studies,[15,16] we show the relationship between the cosine of the contact angle and the curvature of the contact line that our MD results produce in Fig. 2. Note that the contact radius is normalized by σ_O for clarity. Based on linear fits to the two series of data in Fig. 2, the line tensions are determined as 1.23×10^{-11} J/m and 4.75×10^{-11} J/m for the hydrophobic and hydrophilic cases, respectively. The line tension is predicted to be positive, which means that smaller water droplets shrink on the surface and have a larger contact angle. The magnitudes of the line tensions are of the same order as those reported by Werder *et al.*[15] for water droplets

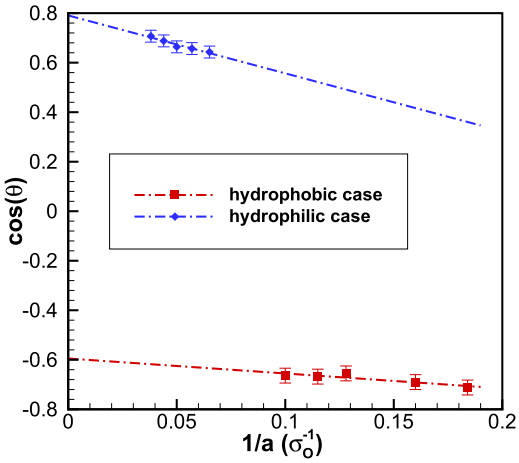

FIG. 2. Cosine of the contact angle θ as a function of the curvature of the contact line ($1/a$) for simulated water droplets. The red squares are data for the hydrophobic surface; blue diamonds are data for the hydrophilic surface. The dotted-dashed lines are linear fits to the data points in each case, and the apparent line tensions are determined from their slopes.

on graphite, where the line tensions were always positive, no matter how large the interaction strength between water and graphite. On the other hand, Barisik and Beskok[25] investigated water droplets on silicon surfaces and found that the line tension is positive for the hydrophobic case but negative for the hydrophilic case. These results demonstrate that the line tension is dependent not only on the wetting properties but also on the surface materials themselves and their lattice structures.

It should be noted that the characteristic radii of the water droplets at equilibrium in our simulations are several nanometers. At such a small scale, the effect of the curvature on the liquid-vapour surface tension becomes important, and this results in the surface tension of a droplet deviating from its planar value. According to previous theoretical analyses and experiments, the curvature-dependent surface tension can be written as follows (and neglecting other terms above the first order):[39,40]

$$\gamma_{lv}(R) = \gamma_\infty\left(1 - \frac{2\delta^T}{R}\right), \tag{5}$$

where R is the droplet radius, γ_∞ denotes the liquid-vapour surface tension of a complete flat surface, and δ^T is the Tolman length. Replacing the surface tension of a flat surface γ_∞ used in Eq. (2) by the curvature-dependent surface tension $\gamma_{lv}(R)$ defined in Eq. (5), we obtain

$$\cos\,\theta = \cos\,\theta_Y - \frac{1}{\gamma_\infty a}(\tau^* - \delta^T\gamma_\infty \sin\,2\theta_Y). \tag{6}$$

It can be seen that the line tension τ in Eq. (2) is replaced by $\tau^* - \delta^T\gamma_{lv}\sin 2\theta_Y$ in Eq. (6). Therefore, we can still use a line fit to the relation of the cosine of the contact angle to the curvature of the contact line; the only change is that the slope of the fitting line is $-(\tau^* - \delta^T\gamma_{lv}\sin 2\theta_Y)/\gamma_\infty$ instead of $-\tau/\gamma_\infty$. For the sake of comparison, we refer to τ in Eq. (2) as the apparent line tension and τ^* in Eq. (6) as the modified line tension that incorporates the effect of Tolman length. Note that other effects are still included in τ^*, so it is not a pure line tension; our aim here is to study how the Tolman length affects the measured line tension, rather than to obtain a value of the pure line tension.

By comparing Eqs. (2) and (6), a simple relationship between the modified and apparent line tensions is

$$\tau^* = \tau + \delta^T\gamma_\infty \sin\,2\theta_Y. \tag{7}$$

Despite the controversies about the value and even the sign of the Tolman length in the past, recent experimental[41] and theoretical studies[30,42] approach a consistent value of −0.05 nm for the water-vapour interface. A negative Tolman length means that a convex curved surface tends to flatten itself. According to our previous MD studies,[33] the liquid-vapour surface tension of a flat water surface using the TIP4P/2005 water model at 300 K is 63.9 mN m^{-1}. We use these two values for the Tolman length and surface tension in Eq. (7) to determine the modified line tension.

As the Tolman length is negative, the modified line tension is smaller (larger) than the apparent line tension when the Young's contact angle θ_Y is in the range 0°–90° (90°–180°). Using Eq. (7), we determine that the modified line tensions in the two series of data are 1.53×10^{-11} J/m and 4.44×10^{-11} J/m for the hydrophobic and hydrophilic cases, respectively. The differences between the modified and the apparent line tensions are 25.0% and 6.6% for the hydrophobic and hydrophilic cases, respectively, which means that the Tolman length plays an important role in the measured line tension.

Besides our results (pink circles) in Fig. 3, we include other reported MD results for the apparent line tensions of water droplets on a variety of surfaces. The green squares represent the results of water droplets on graphite obtained by Werder *et al.*,[15] the blue triangles represent the results of water droplets on graphene obtained by Włoch *et al.*,[43] and the red diamonds represent the results of water droplets on silicon obtained by Barisik and Beskok.[25] The corresponding modified line tensions determined using Eq. (7) are also shown as black symbols for comparison. It can be seen that the differences between the apparent and the modified line tensions are

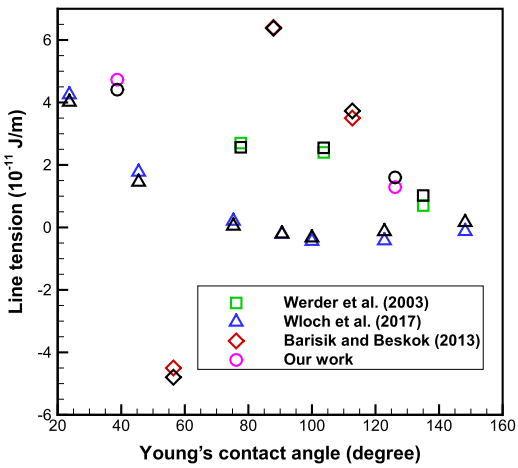

FIG. 3. Comparison of apparent and modified line tensions for water droplets on a variety of surfaces. Apparent line tension: green squares denote water droplets on graphite (Werder *et al.*); blue triangles denote water droplets on graphene (Wloch *et al.*); red diamonds denote water droplets on silicon (Barisik and Beskok); pink circles denote our work for water droplets on platinum. Modified line tension: black symbols for the corresponding data.

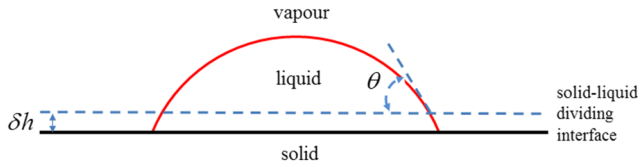

FIG. 4. A sessile liquid droplet on a planar solid surface. The solid black line denotes the position of the topmost layer of substrate atoms, and the dashed line denotes the solid-liquid dividing interface, where the contact angle is measured.

negligible when the Young's contact angle is close to 90°, while the differences are larger if the surfaces are very hydrophilic or hydrophobic. The maximum relative error between the apparent and modified line tensions is up to 232% for the case of water on graphene with a contact angle of 148.2°. In such cases, the effect of the Tolman length needs to be considered for the evaluation of line tension.

All the data, including our results, presented in Fig. 3 are scattered and span a wide range from -4.5×10^{-11} J/m to 6.4×10^{-11} J/m. There is no clear relationship between the line tensions and the wetting properties (Young's contact angle). This indicates that, besides the Tolman length, other effects are important.

B. Effect of the solid-liquid dividing interface

Even for water droplets on graphite surfaces, the line tensions reported by different research groups using MD are quite scattered and are either positive or negative.[15,26,27] Besides the Tolman length, the position of the solid-liquid dividing interface might be an important factor for the scattering of the measured line tensions. In this subsection, we choose different solid-liquid dividing interfaces and check how these change the contact angle and the line tension. As illustrated in Fig. 4, the solid-liquid dividing interface is set at δh above the topmost layer of substrate atoms. We obtained MD results for $\delta h = \sigma_O$ and $\delta h = 2\sigma_O$ to compare with the results for $\delta h = 0$ presented in Fig. 2.

As shown in Fig. 5, different solid-liquid dividing interfaces produce different contact angles for the water droplets

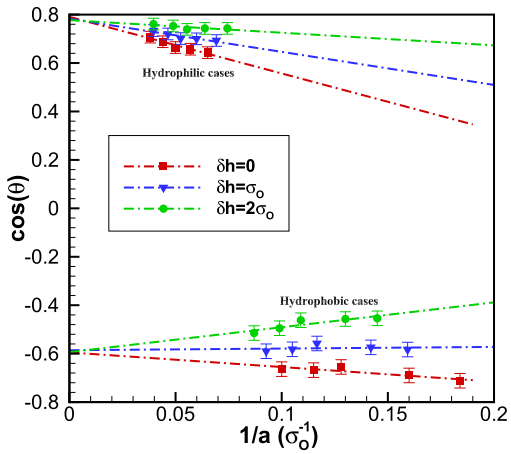

FIG. 5. Comparison of results for different solid-liquid dividing interfaces for water droplets; δh is the distance from the topmost layer of solid substrate atoms to the user-defined solid-liquid dividing interface.

on the platinum surface. Consequently, the apparent line tension determined by a linear fitting is dependent on the interface location. Specifically, for the hydrophobic case, the apparent line tension changes from 1.23×10^{-11} J/m with $\delta h = 0$ to -1.38×10^{-12} J/m with $\delta h = \sigma_O$ and -2.08×10^{-11} J/m with $\delta h = 2\sigma_O$; for the hydrophilic case, the apparent line tension changes from 4.75×10^{-11} J/m with $\delta h = 0$ to 2.77×10^{-11} J/m with $\delta h = \sigma_O$ and 1.05×10^{-11} J/m with $\delta h = 2\sigma_O$. As the height of the solid-liquid dividing interface increases, the measured apparent line tension decreases. It is interesting to note that the sign of the measured line tension for the hydrophobic case changes to negative if $\delta h > \sigma_O$. For the hydrophilic case, our results with $\delta h \le 2\sigma_O$ are always positive, but there is a trend toward the measured line tension being negative if δh becomes larger.

These findings may explain the controversial results for the apparent line tension reported in the literature, as it is so sensitive to the position chosen for the solid-liquid dividing interface. A value for the apparent line tension is only meaningful if the solid-liquid dividing interface is also defined. Schimmele *et al.*[28] derived an expression for the difference between two apparent line tensions ($\Delta\tau$) caused by the distance between two arbitrary solid-liquid dividing interfaces (Δh) as follows:

$$\Delta\tau = \gamma_{lv}\Delta h \sin\theta_Y. \tag{8}$$

According to Eq. (8), the differences in two measured apparent line tensions with different solid-liquid dividing interface locations ($\delta h = 0$ and $\delta h = 2\sigma_O$) for hydrophobic and hydrophilic cases are 3.26×10^{-11} J/m and 2.52×10^{-11} J/m, respectively. On the other hand, our MD results presented in Fig. 5 showed that the corresponding differences are 3.31×10^{-11} J/m and 3.70×10^{-11} J/m for the hydrophobic and hydrophilic cases, respectively. It can be seen that the prediction of Eq. (8) and the MD result are quantitatively consistent for the hydrophobic case, while they are in qualitative agreement for the hydrophilic case. Essentially, our MD results provide numerical support to Eq. (8).

To determine the pure line tension, the effects of the Tolman length and the position of the solid-liquid dividing interface must be taken into account simultaneously. Schimmele *et al.*[28] gave a theoretical formula considering these effects as follows:

$$\cos\theta = \cos\theta_Y + \frac{1}{\gamma_{lv}a} \times \left\{\left(2\delta^T\gamma_{lv} - \frac{d\tau}{d\theta}\Big|\right)\sin\theta_Y\cos\theta_Y - \tau' - a\frac{d\tau}{da}\Big|\right\}, \tag{9}$$

where τ' is the pure line tension and $\frac{d\tau}{d\theta}|$ and $\frac{d\tau}{da}|$ are the stiffness coefficients of the contact line. As analyzed by Schimmele *et al.*,[28] while the pure line tension is independent of the dividing interface, the stiffness coefficients represent the dependence of the apparent line tension on the chosen position of the dividing interface.

So far, there have been no MD simulations of three-dimensional droplets to obtain the pure line tension of droplets because the effects of the Tolman length and the stiffness coefficients are coupled, as seen in Eq. (9). Even the two stiffness coefficients themselves $\frac{d\tau}{d\theta}|$ and $\frac{d\tau}{da}|$ are inherently not

distinguishable and can only be investigated simultaneously, making their direct calculation quite difficult. If the effect of the stiffness coefficients is negligible, i.e., $\frac{d\tau}{d\theta}| = 0$ and $\frac{d\tau}{da}| = 0$, then Eq. (9) reverts to Eq. (6).

For the sake of simplicity, Kanduč[30] investigated two-dimensional cylindrical water droplets to study the effect of $\frac{d\tau}{d\theta}|$, while he dismissed the effect of $\frac{d\tau}{da}|$ because the length and the curvature of the three-phase contact line are independent of the droplet size in a cylindrical water droplet. He reported that the stiffness coefficient $\frac{d\tau}{d\theta}|$ makes a contribution to the contact angle comparable to the pure line tension, especially for hydrophilic surfaces.

It should be noted that although the apparent line tension is related to the effects of the Tolman length and the position of the solid-liquid dividing interface, the predicted macroscopic contact angle (at $1/a = 0$ in Fig. 5) is invariant, based on a linear fit of the measured contact angle at the nanoscale and extrapolation to the macroscopic limit. This means that the modified Young's equation is a better tool to predict the macroscopic contact angle, instead of the pure line tension.

IV. CONCLUSIONS

We have employed MD simulations to study three-dimensional nanoscale water droplets on both hydrophobic and hydrophilic surfaces. By simulating different sizes of nanodroplets for each wetting property, we identified the apparent line tension by fitting the cosine of the contact angles to the curvature of the contact line. Our MD simulation results also demonstrated that both the Tolman length and the chosen position of the solid-liquid dividing interface significantly affect the value and even the sign of the measured line tension. A value for the apparent line tension is only meaningful if the location of the solid-liquid dividing interface is also specified. This may explain why previous reported results for the line tension are so scattered. On the other hand, our simulation results demonstrated that the modified Young's equation is a useful tool for predicting the macroscopic contact angle based on a linear fit of the measured contact angles at the nanoscale, although the line tension defined in the modified Young's equation is not the pure line tension but the apparent line tension.

We have considered the effects of the Tolman length and the stiffness coefficients separately, so we have not obtained the pure line tension for three-dimensional droplets. Identifying this is challenging because the pure line tension and the effects of the Tolman length and the stiffness coefficients are entangled, as seen in Eq. (9). Research in this direction would be useful future work.

ACKNOWLEDGMENTS

J.Z. was supported by the National Natural Science Foundation of China (Grant No. 11772034). M.K.B. and J.M.R. were financially supported by the UK's Engineering and Physical Sciences Research Council (EPSRC) under Grant Nos. EP/R007438/1 and EP/N016602/1. J.M.R. is supported by the Royal Academy of Engineering under the Chair in Emerging Technologies scheme. All data within this publication can be freely accessed at http://dx.doi.org/10.7488/ds/2380.

[1] D. Brutin, *Droplet Wetting and Evaporation: From Pure to Complex Fluids* (Academic Press, 2015).
[2] R. N. Dahms, "Understanding the breakdown of classic two-phase theory and spray atomization at engine-relevant conditions," Phys. Fluids **28**, 042108 (2016).
[3] F.-C. Wang, F. Yang, and Y.-P. Zhao, "Size effect on the coalescence-induced self-propelled droplet," Appl. Phys. Lett. **98**, 053112 (2011).
[4] Q. Yuan and Y.-P. Zhao, "Multiscale dynamic wetting of a droplet on a lyophilic pillar-arrayed surface," J. Fluid Mech. **716**, 171–188 (2013).
[5] J. Zhang, F. Leroy, and F. Müller-Plathe, "Influence of contact-line curvature on the evaporation of nanodroplets from solid substrates," Phys. Rev. Lett. **113**, 046101 (2014).
[6] P. Galliker, J. Schneider, H. Eghlidi, S. Kress, V. Sandoghdar, and D. Poulikakos, "Direct printing of nanostructures by electrostatic autofocussing of ink nanodroplets," Nat. Commun. **3**, 890 (2012).
[7] T. Ondarçuhu and J.-P. Aimé, *Nanoscale Liquid Interfaces: Wetting, Patterning and Force Microscopy at the Molecular Scale* (CRC Press, 2013).
[8] D. Bonn, J. Eggers, J. Indekeu, J. Meunier, and E. Rolley, "Wetting and spreading," Rev. Mod. Phys. **81**, 739 (2009).
[9] D. Quéré, "Rough ideas on wetting," Phys. A **313**, 32–46 (2002).
[10] P. Roura and J. Fort, "Local thermodynamic derivation of Young's equation," J. Colloid Interface Sci. **272**, 420–429 (2004).
[11] D. Seveno, T. D. Blake, and J. De Coninck, "Young's equation at the nanoscale," Phys. Rev. Lett. **111**, 096101 (2013).
[12] T. Ingebrigtsen and S. Toxvaerd, "Contact angles of Lennard-Jones liquids and droplets on planar surfaces," J. Phys. Chem. C **111**, 8518–8523 (2007).
[13] J.-C. Fernandez-Toledano, T. Blake, P. Lambert, and J. De Coninck, "On the cohesion of fluids and their adhesion to solids: Young's equation at the atomic scale," Adv. Colloid Interface Sci. **245**, 102–107 (2017).
[14] R. J. Good and M. Koo, "The effect of drop size on contact angle," J. Colloid Interface Sci. **71**, 283–292 (1979).
[15] T. Werder, J. Walther, R. Jaffe, T. Halicioglu, and P. Koumoutsakos, "On the water-carbon interaction for use in molecular dynamics simulations of graphite and carbon nanotubes," J. Phys. Chem. B **107**, 1345–1352 (2003).
[16] J. H. Weijs, A. Marchand, B. Andreotti, D. Lohse, and J. H. Snoeijer, "Origin of line tension for a Lennard-Jones nanodroplet," Phys. Fluids **23**, 022001 (2011).
[17] J. W. Gibbs, *The Collected Works of J. Willard Gibbs*, Thermodynamics Vol. 1 (Yale University Press, 1945).
[18] L. Boruvka and A. Neumann, "Generalization of the classical theory of capillarity," J. Chem. Phys. **66**, 5464–5476 (1977).
[19] T. Getta and S. Dietrich, "Line tension between fluid phases and a substrate," Phys. Rev. E **57**, 655 (1998).
[20] H. Dobbs and J. Indekeu, "Line tension at wetting: Interface displacement model beyond the gradient-squared approximation," Phys. A **201**, 457–481 (1993).
[21] A. Amirfazli and A. Neumann, "Status of the three-phase line tension: A review," Adv. Colloid Interface Sci. **110**, 121–141 (2004).
[22] L.-O. Heim and E. Bonaccurso, "Measurement of line tension on droplets in the submicrometer range," Langmuir **29**, 14147–14153 (2013).
[23] K. Zhang, F. Wang, and X. Zhao, "The self-propelled movement of the water nanodroplet in different surface wettability gradients: A contact angle view," Comput. Mater. Sci. **124**, 190–194 (2016).
[24] R. C. Dutta, S. Khan, and J. K. Singh, "Wetting transition of water on graphite and boron-nitride surfaces: A molecular dynamics study," Fluid Phase Equilib. **302**, 310–315 (2011).
[25] M. Barisik and A. Beskok, "Wetting characterisation of silicon (1, 0, 0) surface," Mol. Simul. **39**, 700–709 (2013).
[26] R. Ramírez, J. K. Singh, F. Müller-Plathe, and M. C. Böhm, "Ice and water droplets on graphite: A comparison of quantum and classical simulations," J. Chem. Phys. **141**, 204701 (2014).
[27] D. Sergi, G. Scocchi, and A. Ortona, "Molecular dynamics simulations of the contact angle between water droplets and graphite surfaces," Fluid Phase Equilib. **332**, 173–177 (2012).
[28] L. Schimmele, M. Napiórkowski, and S. Dietrich, "Conceptual aspects of line tensions," J. Chem. Phys. **127**, 164715 (2007).
[29] L. Schimmele and S. Dietrich, "Line tension and the shape of nanodroplets," Eur. Phys. J. E **30**, 427 (2009).

[30]M. Kanduč, "Going beyond the standard line tension: Size-dependent contact angles of water nanodroplets," J. Chem. Phys. **147**, 174701 (2017).
[31]S. M. Longshaw, M. K. Borg, S. B. Ramisetti, J. Zhang, D. A. Lockerby, D. R. Emerson, and J. M. Reese, "mdFoam+: Advanced molecular dynamics in openfoam," Comput. Phys. Commun. **224**, 1–21 (2018).
[32]K. Ritos, N. Dongari, M. K. Borg, Y. Zhang, and J. M. Reese, "Dynamics of nanoscale droplets on moving surfaces," Langmuir **29**, 6936–6943 (2013).
[33]J. Zhang, M. K. Borg, K. Sefiane, and J. M. Reese, "Wetting and evaporation of salt-water nanodroplets: A molecular dynamics investigation," Phys. Rev. E **92**, 052403 (2015).
[34]J. Zhang, M. K. Borg, K. Ritos, and J. M. Reese, "Electrowetting controls the deposit patterns of evaporated salt water nanodroplets," Langmuir **32**, 1542–1549 (2016).
[35]J. Zhang, M. K. Borg, and J. M. Reese, "Multiscale simulation of dynamic wetting," Int. J. Heat Mass Transfer **115**, 886–896 (2017).
[36]J. L. Abascal and C. Vega, "A general purpose model for the condensed phases of water: TIP4P/2005," J. Chem. Phys. **123**, 234505 (2005).
[37]H. Peng, A. V. Nguyen, and G. R. Birkett, "Determination of contact angle by molecular simulation using number and atomic density contours," Mol. Simul. **38**, 945–952 (2012).
[38]M. Foroutan, S. M. Fatemi, F. Esmaeilian, V. Fadaei Naeini, and M. Baniassadi, "Contact angle hysteresis and motion behaviors of a water nanodroplet on suspended graphene under temperature gradient," Phys. Fluids **30**, 052101 (2018).
[39]R. C. Tolman, "The effect of droplet size on surface tension," J. Chem. Phys. **17**, 333–337 (1949).
[40]H. M. Lu and Q. Jiang, "Size-dependent surface tension and Tolman's length of droplets," Langmuir **21**, 779–781 (2005).
[41]M. E. M. Azouzi, C. Ramboz, J.-F. Lenain, and F. Caupin, "A coherent picture of water at extreme negative pressure," Nat. Phys. **9**, 38 (2013).
[42]M. N. Joswiak, R. Do, M. F. Doherty, and B. Peters, "Energetic and entropic components of the Tolman length for mW and TIP4P/2005 water nanodroplets," J. Chem. Phys. **145**, 204703 (2016).
[43]J. Włoch, A. P. Terzyk, and P. Kowalczyk, "New forcefield for water nanodroplet on a graphene surface," Chem. Phys. Lett. **674**, 98–102 (2017).